Available online at www.sciencedirect.com
ScienceDirect
Nuclear and Particle Physics Proceedings 273–275 (2016) 295–301
www.elsevier.com/locate/nppp

The status of KIMS-NaI experiment

Hyun Su Lee on behalf of the KIMS collaboration

Department of Physics, Ewha Womans University, Seoul 120-750, Korea

Abstract

Among the direct searches for WIMP-type dark matter, the only DAMA experiment has consistently reported a positive signal for an annual-modulation signal with a large (9.3σ) statistical significance. Even though many compelling experiments have reported controversial results that report null signals in the DAMA signal region, there is a room to explain all of these results without conflict due to differences of detector as well as astronomical model. This necessitates an independent verification of the origin of the observed modulation signal using the same technique as that employed by the DAMA experiment. The KIMS-NaI experiment aim the reproducing the DAMA signals with same detector, NaI(Tl) crystal. Here, we report first results of a program of NaI(Tl) crystal measurements at the Yangyang Underground Laboratory.

1. Introduction

Numerous astronomical observations have led to the conclusion that most of the matter in the Universe is invisible, exotic, and nonrelativistic dark matter [1, 2]. However, in spite of a considerable amount of experimental effort, the nature of the dark matter remains unknown. Weakly interacting massive particles (WIMPs) are one of the most attractive candidates for dark matter particles [3, 4]. In supersymmetric models for beyond the standard model physics, the lightest supersymmetric particle (LSP) is a natural candidate for WIMP-type dark matter. A number of experiments have made direct searches for a WIMP component of our Galaxy by looking for evidence for WIMP-nucleus scattering by detecting the recoiling nucleus in ultra-sensitive low-background detectors [5, 6].

The DAMA experiment searches for an annual modulation in the detection rate of nuclear recoils in an array of ultra-low-background NaI(Tl) crystals caused by the Earth's orbital motion through our Galaxy's dark-matter halo [7, 8, 9]. This experiment, which has been operating for over 15 years, has consistently reported a positive signal for an annual modulation with a phase that is consistent with expectations for motion of the Earth relative to the Galactic rest frame. The statistical significance of the DAMA annual modulation signal has now reacehed 9.3σ. The DAMA signal, in particular its interpretation as being due to WIMP-nucleus scattering, has been the subject of a continuing debate that started with the first DAMA report 15 years ago. This is because the WIMP-nucleon cross sections inferred from the DAMA modulation are in conflict with limits from other experiments that directly measure the total rate of nuclear recoils, such as XENON100 [10], LUX [11], and SuperCDMS [12]. However, room remains for explaining all of these experimental results without conflict in terms of nontrivial systematic differences in detector responses [13, 14] and the commonly used astronomical model for the WIMP distribution [15]. An unambiguous verification of the DAMA signal by an independent experiment using similar NaI(Tl) crystals is mandatory.

Reproducing the DAMA measurement requires the independent development of ultra-low-background NaI(Tl) crystals. This is because the crystal-growing company that supplied the DAMA NaI(Tl) crystals will

http://dx.doi.org/10.1016/j.nuclphysbps.2015.09.041

not produce the same crystals for other experimental groups. Recently, the ANAIS group has been developing ultra-low-background NaI(Tl) crystals with the goal of reproducing the DAMA result [16, 17] and the DM-Ice group reports background measurements of NaI(Tl) crystals [18]. However, to date, no experimental group has produced NaI(Tl) crystals with background levels at or below than those used in the DAMA experiment. Here, we report first results of KIMS-NaI program at Yangyang underground laboratory [19].

2. Experimental Setup

To evaluate the NaI(Tl) crystals, we use the experimental setup that was used for the KIMS CsI(Tl) detector measurements [20, 21, 22] at the Yangyang Underground Laboratory (Y2L), which has a 700 m earth overburden (2400 m water equivalent). This includes a 12-module array of CsI(Tl) detectors (total mass of 103.4 kg) inside a shield that consists, from inside out, of 10 cm of copper, 5 cm of polyethylene, 15 cm of lead, and 30 cm of liquid-scintillator-loaded mineral oil to stop external neutrons, gamma rays, and veto cosmic ray muons. Each detection module consists of a low-background CsI(Tl) crystal ($8 \times 8 \times 30$ cm^3) with a photomultiplier tube (PMT) mounted at each end.

Two NaI(Tl) crystals were mounted inside the CsI(Tl) detector array. In November 2013, we installed the first NaI(Tl) crystal, NaI-001, in the CsI array; the second NaI(Tl) crystal, NaI-002, was added in February 2014, soon after that crystal was delivered and assembled.

The two NaI(Tl) crystals were produced by the Alpha Spectra Company. The crystals were grown from NaI powder that was not of the highest attainable purity; the initial purification was carried out by Alpha Spectra. The crystals have a cylindrical shape and were cut from a 32 inch ingot that was grown by the Kyropoulos method. After the crystal surfaces were polished they were wrapped with a Teflon reflector and inserted into an oxigen-free electronic (OFE) copper cylinder and encapsulated in a nitrogen gas environment. There is a 12.7-mm-thick quartz-plate window at each end of the cylinder, with optical grease between the crystal and the quartz windows. A 3″ PMT is mounted at each end of the cylinder.

Each NaI crystal PMT signal was split and amplified by factors of 30 and 2; the amplified signals were digitized by 400- and 64-MHz flash analog-to-digital converters (FADC), respectively. The corresponding amplification factors for the CsI crystal PMTs were ×100 and ×10. The total recorded time window for an event was 40 μs, of which 5 μs is analyzed for the NaI(Tl) crystals and 25 μs is analyzed for the CsI(Tl) crystals, reflecting the different decay times of the two materials.

The trigger condition for the CsI(Tl) crystals is two or more photoelectrons (PEs) in each PMT within a 2-μs time window. The NaI(Tl) crystals have a reduced PE requirement of one PE in each PMTs within a 200 ns window in order to have a minimal trigger bias and a low energy threshold.

3. Signal Calibrations

The energy calibration of the NaI(Tl) crystals was done with a ^{241}Am source. The detector had one hole of 10 mm in diameter covered by 127-μm-thick aluminum foil in the center of the encapsulating Cu container. The source was located in front of the hole. The CsI(Tl) crystal calibration procedure is described in Refs. [20, 21].

For low-energy events, the 400-MHz FADC waveforms were analyzed to identify clusters of single PEs (SPEs) [23]. The charge distribution of a SPE, obtained by identifying isolated clusters at the decay tail of the signal (2–5 μs after the signal start) in order to suppress multiple PE clusters, is shown in Fig. 1. The mean number of PEs, which is estimated as about 15 PE/keV, is calculated with total charge of 59.54 keV peak of ^{241}Am source. This number is consistent with the ANAIS test [16].

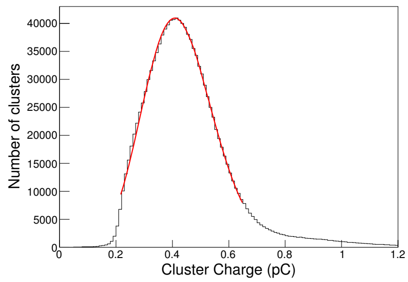

Figure 1: The SPE charge distribution measured with the NaI-001 crystal readout by an R12669 PMT. This distribution is produced with a ^{241}Am calibration source in a time window that is 2–5 μs after the signal start to reduce PE pileup.

4. Natural background

To produce ultra-low-background crystals, contamination from internal natural radioisotopes has to be reduced. Table 1 shows the measured results of the internal backgrounds for the two crystals.

Table 1: Backgrounds from the internal radioactive contaminants in the NaI(Tl) crystals. The units for all the values are mBq/kg. For "Total alphas," each alpha particle is counted as one decay.

Radionuclei	NaI-001	NaI-002
^{238}U (by ^{214}Bi)	<0.0003	<0.0015
^{228}Th (by ^{216}Po)	<0.013	0.002 ± 0.001
^{40}K	1.25 ± 0.09	1.49 ± 0.07
^{210}Pb	3.28 ± 0.01	1.76 ± 0.01
Total alphas	3.29 ± 0.01	1.77 ± 0.01

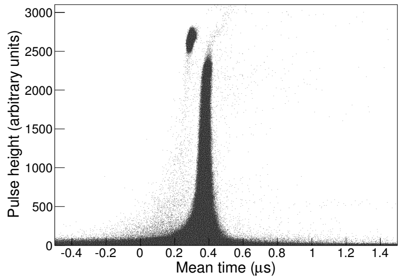

Figure 2: A scatter plot of maximum height *versus* mean time of event signals from NaI-001. Alpha-induced events are well separated from γ-induced signals because of their shorter decay time.

The most serious internal background contamination is ^{40}K because of the low-energy x-ray that is produced during its electron capture decay process, which proceeds via a transition to an excited state of ^{40}Ar with a branching ratio of 10%. This decay generates a ~3 keV x-ray in coincidence with a 1460 keV γ-ray. If the accompanying 1460 keV γ-ray escapes from the crystal, the event consists of a single 3 keV hit. The ^{40}K level in the DAMA crystals is in the 10–20 ppb range [24].

We studied coincidence signals between NaI (~3 keV) and CsI (1460 keV) detectors to identify unambiguous ^{40}K decays. The event cluster near 3 keV in NaI and 1460 keV in a surrounding CsI crystal is identified to estimate ^{40}K contamination. By comparing the rate for ^{40}K induced events with a Geant4-based detector simulation [25] for the CsI and NaI crystal setup, we determine the ^{40}K contamination in the NaI crystals to be 41.4±3.0 ppb (1.25±0.09 mBq/kg) and 49.3±2.4 ppb (1.49±0.07 mBq/kg), respectively, for NaI-001 and NaI-002. This is close to the ^{40}K levels measured in the ANAIS-25 crystals [16, 26].

Although the PMTs are nonlinear at high light output, alpha-induced events inside the crystal can be identified by the mean time of the signal, defined as

$$\langle t \rangle \equiv \frac{\sum_i A_i t_i}{\sum_i A_i}. \quad (1)$$

Here A_i and t_i are the charge and time of each cluster (for low energies) or digitized bin (for high energies). Figure 2 shows a scatter plot of the pulse height *versus* mean time for event signals from NaI-001. Alpha-induced events are clearly separated from gamma-induced events in the high-energy region because of the faster decay times of alpha-induced signals.

Because of the nonlinearity of high-energy signals, alpha particles from different nuclides cannot be distinguished event-by-event by their measured energies. Instead we determine the level of ^{238}U chain contaminants by exploiting the ^{214}Po 237 μs mean lifetime that occurs between ^{214}Bi β-decay and ^{214}Po α-decay, a technique that was used successfully for contamination measurements in the KIMS CsI crystals [27]. Since there is no significant exponential component observed with the 237-μs decay time of ^{214}Po, an upper limit on the activity level is determined. This analysis shows that the contamination levels from the ^{238}U chain are already sufficiently low for a WIMP dark matter search.

Contamination from the ^{232}Th chain is studied by using $\alpha-\alpha$ time interval measurements in the crystals. In this case we look for a ^{216}Po α-decay component with a mean time of 209 ms following its production via ^{220}Rn $\rightarrow$ ^{216}Po α-decay. These $\alpha-\alpha$ event rates can translate into contamination levels from the ^{228}Th series in the ^{232}Th chain. The ^{232}Th contamination levels of the two crystals, listed in Table 1, are also sufficiently low.

The levels of ^{238}U and ^{232}Th contamination measured in both crystals are too low to account for the total observed alpha particle rate, which suggests that they are due to decays of ^{210}Po nuclei that originate from ^{222}Rn contamination that occured sometime during the powder and/or crystal processing stages. This is confirmed by the observation of a 46-keV γ peak that is characteristic of ^{210}Pb.

The time change in the total alpha rate provides information about when the ^{222}Rn contamination occurred. After ^{222}Rn contamination, the number of ^{210}Pb nuclei increases as does the ^{210}Po α-decay rate. After about three years, equilibrium is reached and the ^{210}Po activity becomes constant. The NaI-001 and NaI-002 crystals emit about 2344 and 1334 alpha particles per day, respectively. After considering the crystal masses, we find that the NaI-002 alpha activity is less than that for NaI-001 by almost a factor of two. Moreover, we also see that the NaI-002 crystal's alpha activity is increasing with time.

For ^{210}Po, the alpha activity will increase as

$$R_\alpha(t) \approx A(1 - e^{-(t-t_0)/\tau_{Po}}), \quad (2)$$

where τ_{Po} is the decay time of ^{210}Po (200 days) and t_0 is the time the initial ^{210}Pb contamination occurred, assuming that the contamination happened suddenly. The measured alpha rate was fitted to this equation, and the results indicate that the contamination occurred at the end of April, 2013. This coincides with the time that the crystal was grown, and we conclude that the contamination occurred then.

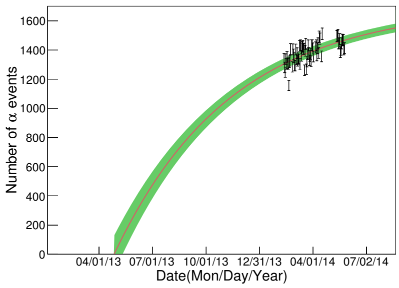

Figure 3: The alpha activity increase in NaI-002 is fitted with a model in which a nearly instantaneous ^{210}Pb contamination is assumed.

5. Background from cosmic excitation

The two crystals were transported from the U.S. to Korea by different means, NaI-001 by air and NaI-002 by sea, in order to understand the cosmogenic-activation-dependence on the delivery method. We have checked the energy spectra difference of each crystal during the first week and for a week-long period after a two-month delay. Figure 4 shows the difference between the first and second measurements. We found a peak at 68.7-keV which is the sum of γ-rays and x-rays from ^{125}I electron capture decay. Identified lower energy peak also can be originated from iodine and tellurium excitation. We found significantly lower cosmogenic activation in the NaI-002 crystal, and we conclude that surface transportation is mandatory for low-background crystals.

6. PMT noise background

The DAMA group reported a signal selection criteria for efficiently removing the PMT noise events from their NaI(Tl) detectors that exploits the fact that noise pulses

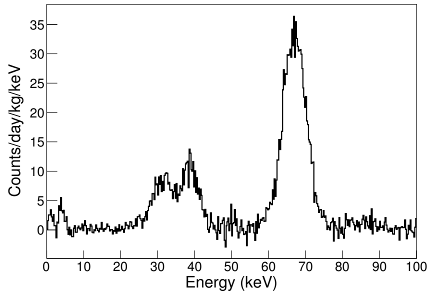

Figure 4: The difference between the initial a week and the 64 day delayed week energy spectra, which shows short life-time cosmogenic activations.

are generally fast. The DAMA requirement places restrictions on the ratio of "fast" charge (0–50 ns), X1, and "slow" charge (100–600 ns), X2 [24, 28]. We examined the DAMA parameters for our NaI(Tl) crystals. Figure 5 shows a two-dimensional X2 *versus* X1 scatter-plot for events in the 2–4 keV energy range both for background data (a) and for data taken with an ^{55}Fe source (b). The figure shows that our discrimination between noise and signal is very efficient, similar to the DAMA results [24]. A rejection rate of the 2–4 keV WIMP search data is approximately 84%, however approximately 86% of the ~3 keV ^{40}K coincidence events is remained.

Although a large fraction of PMT noise events below 5 keV are removed by the DAMA requirement, we find that some PMT noiselike events remain. We, therefore, developed further requirements to remove these events. We first check asymmetry of two PMT signals which allows us to locate where the event occurred inside the crystal. A similar study of asymmetry cuts with NaI crystals was reported previously [29].

To characterize PMT noiselike events, we used multiple hit events in which two or more detector modules satisfy the trigger condition. After applying the DAMA requirement, we compare the asymmetry of two PMTs between the single-hit events and the multiple-hit events. We found that the multiple-hit events are centered, while many single-hit events with energy below 3 keV have asymmetries that are even larger than those for real events that occur near the edge of the crystal. This suggests that these events are caused by visible light produced near one of the PMTs.

We found a peculiar class of low energy events in the single hit sample that are made up of SPE clusters that are spread nearly uniformly over a few hundred nanosecond interval. These are evident in the scatter-

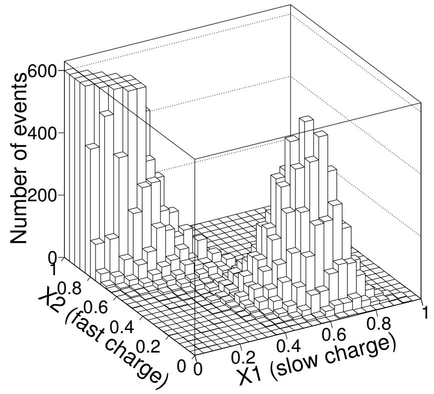

(a) Background data

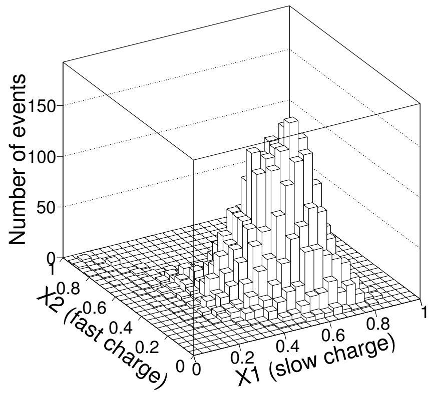

(b)^{55}Fe calibration data

Figure 5: Two-dimensional plots of "fast" and "slow" charges for background (a) and low-energy x-ray source calibration (b) data. PMT noise events have larger "fast" charges and signal events have larger "slow" charges.

plot of the total energy *versus* the average charge of the energy clusters (total charge/number of clusters) shown in Fig. 6, where the black dot entries are for single-hit events and the red circles are for multiple-hit events. A distinct cluster of low energy signals with an average cluster charge consistent with that for a SPE shows up for single-hit events. While the source of these events is still not understood, since they do not show up in multiple hit events, they are considered likely to be induced by PMT-noise. Although this phenomenon requires additional study, for now we veto events that lie to the left of the solid curve shown in the figure.

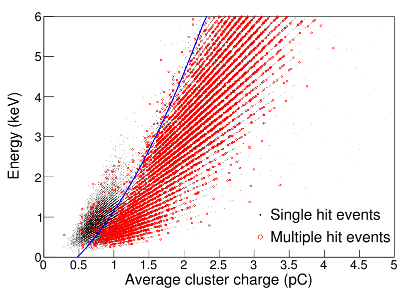

Figure 6: Energy versus the average charge of clusters for single-hit events (dots) and multiple-hit events (open circles). There are additional noise events for the single-hit events in lower cluster charge regions. The solid line shows the cut condition to remove such noise events.

7. Background model

Figure 7 shows the background levels of the two crystals coupled to R12669 PMTs after the application of all of the event selection criteria discussed before. NaI-002 has a much lower background level than that of NaI-001, because of its lower cosmogenic activation as a result of its surface delivery and its lower ^{210}Pb contamination. Its background level at 6 keV is ~3 counts/kg/keV/day. The figure also shows that the new PMTs with higher quantum efficiency may enable us to lower the energy threshold to near 1 keV if we have an additional understanding of the PMT noise below 2 keV.

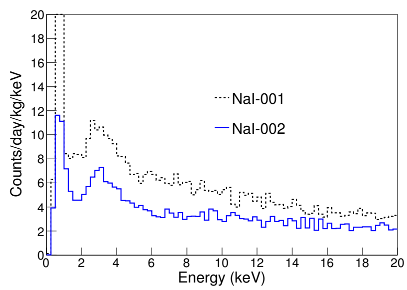

Figure 7: Background levels in the two crystals after the application of the PMT noise rejection requirements. Here we show data obtained with the R12669 glass PMTs.

We simulated the background spectra with Geant4-based detector simulations of ^{210}Pb, ^{238}U, ^{232}Th, and ^{40}K with contamination levels set at the measured values for each crystal.shows the data and the simulated spectra for the NaI-002 crystal. For the current NaI(Tl) crystals, the significant remaining backgrounds are from ^{210}Pb, ^{40}K, and PMT noise. The U, Th, and Ra internal contamination levels in the crystal produce backgrounds at low energies that are already sufficiently small: *i.e.* <0.1 counts/keV/kg/day. The measured background levels of NaI crystals for energies below 10 keV is higher than that of the internal background simulation by ~2 counts/keV/kg/day. This difference is attributed to γ-rays from sources that are exterior to the crystal, *i.e.*, the PMTs, the surrounding CsI crystals, and the materials of the surrounding shield. In addition to these constant backgrounds, there are also ^{125}I and ^{125}Te cosmogenic backgrounds that are continuously decreasing as a function of time. Further simulations will clarify and quantify the contributions from each external source as well as the contributions from cosmogenic activations to the total background level.

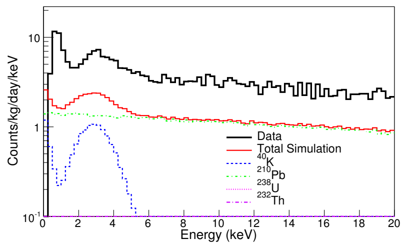

Figure 8: The measured background levels in the NaI-002 crystal compared with simulations of backgrounds from internal contamination in the crystals.

8. Pulse shape discrimination

It has been known that pulse shape discrimination (PSD) of NaI(Tl) crystal between nuclear recoil signals and electron recoil events is much poorer than that of CsI(Tl) crystal [30, 31, 32]. However, due to the large light yield of current NaI(Tl) crystal, we may expect much better PSD of the current NaI(Tl) crystal than that of previous one. We measure PSD performance of a small test crystal ($2.0 \times 2.0 \times 1.5$ cm^3) that was cut from same ingot of NaI-001 crystal using a 300 mCi Am-Be neutron source facility [32]. To characterize a power of PSD performance, we use quality factor suggested in Ref. [33]. Figure 9 present the measured qaulity factors of the NaI(Tl) crystal compared with previous measurement of NaI(Tl) crystal [30] as well as those from CsI(Tl) crystals [31, 32]. Because lower quality factor means better PSD capability, our crystal (alpha spectra) have approximately one order of magnitude better PSD power than the one used in Ref. [30]. Also, we find a little bit better PSD performance than CsI(Tl) crystals. Considering the PSD capability of the NaI(Tl) crystal, we calcuate expected sensitify assuming detector performances as one can see in Fig 10. If we grow 1 dru background, 2 keV energy threshold, and 100 kg NaI(Tl) detectors, we can fully search the DAMA signal regions with PSD analysis only using 1 year data taking.

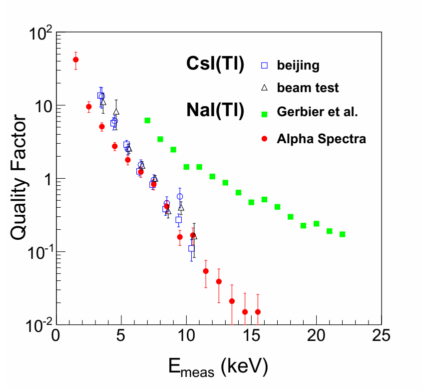

Figure 9: The quality factor of NaI(Tl) crystal (alpha spectra) is compared with previous studies of NaI and CsI crystals.

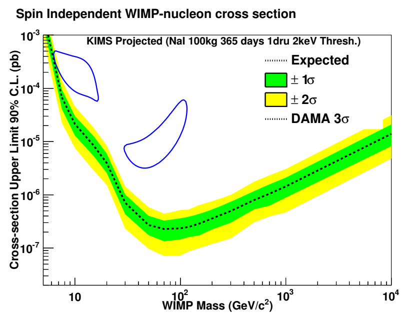

Figure 10: The expected senstivity of KIMS-NaI experiment with 100 kg NaI(Tl) crystal, 1 dru background, 2 keV energy threshold running 1 year data taking is calculated with the measured PSD power.

9. Perspectives

The DAMA experiment has been consistently showing a significant annual modulation with two different experimental arrangements that has persisted over the past 15 years. To check these results, it is necessary to use the same target material and preferable to have a lower threshold and reduced background levels. Achieving a software energy threshold of 1 keV seems feasible because of the high crystal light output and the high quantum efficiency of the new PMTs. Background levels can be significantly improved from the current measured background level of ∼3 counts/keV/kg/day (at 6 keV) by growing the crystals from purer NaI powder and in a Rn-free environment. Because the main internal backgrounds are due to ^{210}Pb and ^{40}K, we are attempting to reduce these contaminations below the background level of 0.2 counts/keV/kg/day for each source, and the prospects of starting with purer powder from Sigma Aldrich are promising.

In addition to the internal backgrounds, the external backgrounds need to be controlled well below 0.5 counts/keV/kg/day. Low-background, metal-housed PMTs with lower radioactivity specifications are commercially available and it is possible to use high efficiency SBA photocathodes with these tubes. We are working closely with the Hamamatsu Company to develop a PMT that is better suited for a low-background NaI(Tl) crystal detector module.

Further, we expect a significant reduction in the internal or external backgrounds by the immersion of the NaI(Tl) crystal array inside a liquid scintillator box that provides an active veto capability. A naive simulation shows that ∼70% of the PMT-initiated backgrounds below 10 keV can be vetoed. A performance test with a single NaI crystal is in progress.

10. Conclusion

We tested the performance of two large NaI(Tl) crystals as part of a program to develop ultra-low-background NaI crystals for WIMP searches. We developed selection requirements that are effective for reducing PMT-noise induced background signals. Based on this effort, we achieved a background level of ∼3 counts/keV/kg/day at 6 keV and a <2 keV energy threshold. A number of efforts are being pursued that are aimed at further reduction of these backgrounds. The successful development of ultra-low-background and low-energy-threshold NaI crystals with much reduced PMT background will guarantee a definitive and unambiguous test of the DAMA experiment's annual modulation signal.

Acknowledgments

We thank the Korea Hydro and Nuclear Power (KHNP) company for providing the underground laboratory space at Yangyang. This research was funded by Grant No. IBS-R016-D1 and was supported by the Basic Science Research Program through the National Research Foundation of Korea (NRF) funded by the Ministry of Education (NRF-2011-35B-C00007).

[1] E. Komatsu *et al.* (WMAP Collaboration), Astrophys. J. Suppl. 192 (2011) 18.
[2] P. A. R. Ade *et al.* (Planck Collaboration), arXiv:1303.5076.
[3] B. W. Lee and S. Weinberg, Phys. Rev. Lett. 39 (1977) 165.
[4] G. Jungman, A. Kamionkowski, and K. Griest, Phys. Rep. 267 (1996) 195.
[5] R. Gaitskell, Annu. Rev. Nucl. Part. Sci. 54 (2004) 315.
[6] L. Baudis, Phys. Dark Univ. 1 (2012) 94.
[7] R. Bernabei *et al.* (DAMA Collaboration), Eur. Phys. J. C 56 (2008) 333.
[8] R. Bernabei *et al.* (DAMA Collaboration), Eur. Phys. J. C 67 (2010) 39.
[9] R. Bernabei *et al.* (DAMA Collaboration), Eur. Phys. J. C 73 (2013) 2648.
[10] E. Aprile *et al.* (XENON100 Collaboration), Phys. Rev. Lett. 109 (2012) 181301.
[11] R. Agnese *et al.* (SuperCDMS Collaboration), Phys. Rev. Lett. 112 (2014) 041302.
[12] D. S. Akerib *et al.* (LUX Collaboration), Phys Rev. Lett. 112 (2014) 091303.
[13] G. Plante *et al.* , Phys Rev. C 84 (2011) 045805.
[14] D. Barker and D. M. Mei, Astropart. Phys. 38 (2012) 1.
[15] Y. Y. Mao, L. E. Strigari, and R. H. Wechsler, Phys. Rev. D 89 (2014) 063513.
[16] J. Amare *et al.*, Nucl. Instrum. Methods Phys. Res., Sect. A 742 (2014) 187.
[17] J. Amare *et al.*, arXiv:1404.3564.
[18] J. Cherwinka *et al.* (DM-Ice Collaboration), arXiv:1401.4804.
[19] K. W. Kim *et al.*, arXiv:1407.1586, accepted in Astropart. Phys.
[20] H. S. Lee *et al.*, (KIMS Collaboration), Phys. Rev. Lett. 99 (2007) 091301.
[21] S. C. Kim *et al.*, (KIMS Collaboration), Phys. Rev. Lett. 108 (2012) 181301.
[22] H. S. Lee *et al.*, (KIMS Collaboration), Phys. Rev. D 90 (2014) 052006.
[23] H. S. Lee *et al.* (KIMS Collaboration), Phys. Lett. B 633 (2006) 201.
[24] R. Bernabei *et al.*, Nucl. Instrum. Methods Phys. Res., Sect. A, 592 (2008) 297.
[25] S. Agostinelli *et al.*, Nucl. Instrumen. Methods Phys. Res., Sect. A 506 (2003) 250; J. Allison *et al.*, IEEE Tran. Nucl. Sci. 53 (2006) 270.
[26] C. Cuesta *et al.*, arXiv:1403.3580.
[27] T. Y. Kim *et al.*, Nucl. Instrum. Methods Phys. Res., Sect. A 500 (2003) 337; H. S. Lee *et al.*, Nucl. Instrum. Methods Phys. Res., Sect. A 571 (2007) 644.
[28] R. Bernabei *et al.*, JINST 7 (2012) P03009.
[29] M. Robinson *et al.*, Nucl. Instrum. Methods Phys. Res., Sect. A, 545 (2005) 225.
[30] G. Gerbier *et al.*, Astropart. Phys., 11 (1999) 287.
[31] H. Park *et al.*, Nucl. Instrum. Methods Phys. Res., Sect. A, 419 (2002) 460.
[32] H. S. Lee *et al.*, arXiv:1409.0948
[33] R. Gaitskell, Annu. Rev. Nucl. Part. Sci. 54 (2004) 315.